Andrimid producers encode an acetyl-CoA carboxyltransferase subunit resistant to the action of the antibiotic

Xinyu Liu, Pascal D. Fortin*, and Christopher T. Walsh†

Department of Biological Chemistry and Molecular Pharmacology, Harvard Medical School, Boston, MA 02115

Contributed by Christopher T. Walsh, July 15, 2008 (sent for review June 30, 2008)

Andrimid is a hybrid nonribosomal peptide-polyketide antibiotic that blocks the carboxyl-transfer reaction of bacterial acetyl-CoA carboxylase (ACC) and thereby inhibits fatty acid biosynthesis with submicromolar potency. The andrimid biosynthetic gene cluster from *Pantoea agglomerans* encodes an *admT* gene with homology to the acetyl-CoA carboxyltransferase (CT) β-subunit gene *accD*. *Escherichia coli* cells overexpressing *admT* showed resistance to andrimid. Co-overproduction of AdmT with *E. coli* CT α-subunit AccA allowed for the *in vitro* reconstitution of an active heterologous tetrameric CT A_2T_2 complex. A subsequent andrimid-inhibition assay revealed an IC_{50} of 500 nM for this hybrid A_2T_2 in contrast to that of 12 nM for *E. coli* CT A_2D_2. These results validated that AdmT is an AccD homolog that confers resistance in the andrimid producer. Mutagenesis studies guided by the x-ray crystal structure of the *E. coli* A_2D_2 complex disclosed a single amino acid mutation of AdmT (L203M) responsible for 5-fold andrimid sensitivity (IC_{50} = 100 nM). Complementarily, the *E. coli* AccD mutant M203L became 5-fold more resistant in the CT assays. This observation allowed for bioinformatic identification of several *Vibrio cholerae* strains in which *accD* genes encode the Met↔Leu switches, and their occurrences correlate predictively with sensitivities to andrimid *in vivo*.

antibiotic resistance | fatty acid biosynthesis inhibitor

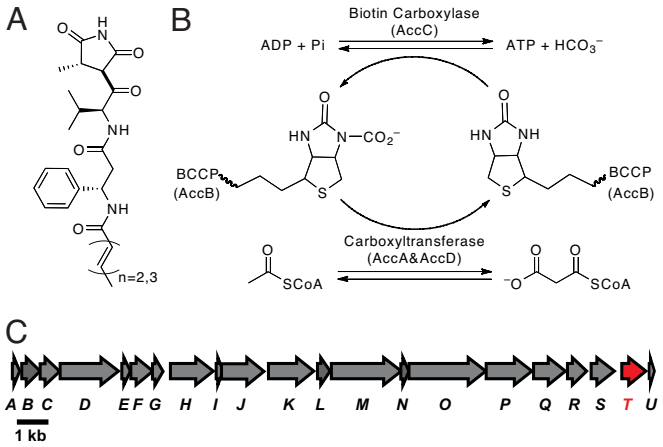

Fig. 1. Antibiotic andrimid and moiramide: structures, molecular target, and biosynthetic gene cluster. (*A*) Structures of andrimid (n = 3) and moiramide (n = 2). Both are potent bacterial ACC inhibitors that target the CT step of the reaction. (*B*) Reaction catalyzed by ACC. In bacteria such as *E. coli*, the BC is encoded by the *accC* gene, whereas BCCP is encoded by the *accB* gene. The two subunits involved in CT activity are encoded by the *accA* (α-subunit) and *accD* (β-subunit) genes. (*C*) The *admT* gene, a homolog of *E. coli accD*, is encoded in the biosynthetic gene cluster of andrimid from *P. agglomerans*.

The inevitable emergence of antibiotic resistance is of major health concern and demands continuous efforts for the discovery of new antibiotics (1). The generation of new classes of antibiotics calls for the identification of novel molecular scaffolds and necessitates detailed understanding of antibiotic–target interactions as well as antibiotic-resistance mechanisms to sustain future developments. Andrimid and moiramide (Fig. 1*A*) belong to a new class of natural antibiotics with a hybrid nonribosomal peptide polyketide scaffold that is acylated at the N terminus and modified by a pyrrolidinedione moiety at the C terminus. Member of this class of pseudopeptidic pyrrolidinedione molecules are widely distributed in nature (2–5) and have received renewed attention when their cellular target was identified to be the bacterial acetyl-CoA carboxylase (ACC) (6). ACC is an essential enzyme that catalyzes the carboxylation of acetyl-CoA to malonyl-CoA, the first committed step of fatty acid biosynthesis (7). The reaction catalyzed by ACC comprises two distinctive half-reactions involving three catalytic components (Fig. 1*B*). Biotin carboxylase (BC) catalyzes the initial step that transfers a carboxyl group to the biotin carboxyl carrier protein (BCCP). The carboxyltransferase (CT) is responsible for the subsequent transfer of the carboxyl group from biotin on the BCCP to acetyl-CoA to form malonyl-CoA. In contrast to mammalian ACCs, where the three enzymatic components reside in a single polypeptide chain (7), bacterial ACC is dissociated into separate subunits. In *Escherichia coli*, monomeric BC and homodimeric BCCP are encoded by *accB* and *accC* genes (8–10), whereas heterotetrameric ($\alpha_2\beta_2$) CT is encoded by *accA* (CT α-subunit) and *accD* (CT β-subunit) genes (Fig. 1*B*) (11, 12). The lack of primary sequence homology between the prokaryote and eukaryote forms of ACC plus their clear structural distinctions have made bacterial ACC a long-appreciated target for antibacterial drug discovery (13). However, no viable medicinal lead was discovered until 2004, when andrimid and moiramide were identified as potent inhibitors of the CT step of the bacterial ACC-catalyzed reactions.

The biosynthetic gene cluster for andrimid in *Pantoea agglomerans* has been identified and sequenced to reveal 21 genes (Fig. 1*C*), the majority of which could be functionally assigned by bioinformatic analyses (14). Subsequent heterologous expression of several ORFs in *E. coli* allowed for the *in vitro* reconstitution of the early biosynthetic pathway and the identification of the function of a transglutaminase homolog, AdmF, as a new condensation catalyst in the enzymatic assembly line (15). The disclosure of the andrimid biosynthetic gene cluster also provided clues on how the andrimid producer acquires immunity to

Author contributions: X.L. and C.T.W. designed the research; X.L. and P.D.F. performed the research; X.L., P.D.F., and C.T.W. analyzed the data; and X.L., P.D.F., and C.T.W. wrote the paper.

The authors declare no conflict of interest.

*Present address: Novartis Institutes for Biomedical Research, Inc., Cambridge, MA 02139.

†To whom correspondence should be addressed at: Department of Biological Chemistry and Molecular Pharmacology, Harvard Medical School, 240 Longwood Avenue, Boston, MA 02115. E-mail: christopher_walsh@hms.harvard.edu.

This article contains supporting information online at www.pnas.org/cgi/content/full/0806873105/DCSupplemental.

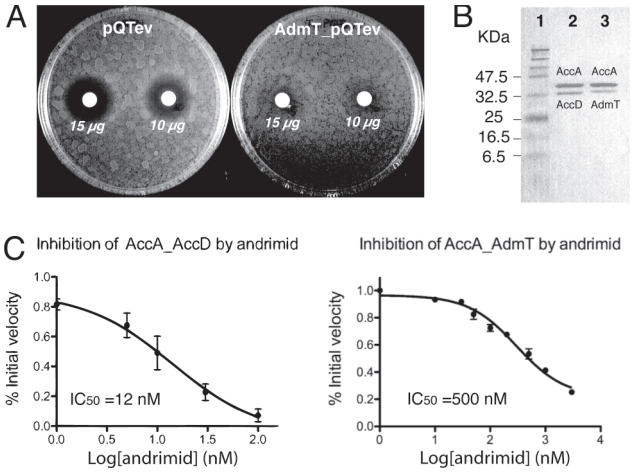

Fig. 2. Functional validation of AdmT. (*A*) Overexpression of AdmT by using expression vector pQTev in *E. coli* confers resistance to andrimid (*Right*), whereas the *E. coli* cell transformed with control pQTev plasmid is sensitive to andrimid (*Left*) (Assay disks were deposited with 10 and 15 μg of andrimid, respectively). (*B*) SDS/PAGE of purified AccD and AdmT co-expressed with His-tagged AccA protein in *E. coli*. Lane 1, molecular markers; lane 2, purified AccA/AccD complex; lane 3, purified AccA/AdmT complex. In both cases, AccA is shown as the top bands. (*C*) *In vitro* inhibition assay of AccA/AccD and AccA/AdmT by andrimid. CT activities are plotted against increasing concentrations of andrimid.

the antibiotic. Previous study showed that the andrimid-sensitive *E. coli* strain became resistant to andrimid when overexpressing *admQ*, which encodes a homolog of major facilitator subfamily transporter responsible for the antibiotic efflux (14).

The penultimate ORF in the andrimid biosynthetic gene cluster is *admT*, a gene that bears homology to *E. coli accD* (Fig. 1*C*). Because andrimid targets bacterial acetyl-CoA CT, we hypothesized that *admT* encodes a resistant form of acetyl-CoA CT β-subunit that thereby acts as a second mechanism for the self-protection of andrimid producers. Here, we report the detailed *in vivo* and *in vitro* biochemical characterization of AdmT that validates our postulation. Mutagenesis studies on AdmT led us to identify key amino acid residues that contribute to the resistance, which subsequently allowed for the prediction of andrimid resistance among other bacterial strains. Overall, this study provides insight into the resistance mechanisms of andrimid and the binding mode of andrimid and moiramide with bacterial acetyl-CoA CT.

Results

Function Validation of AdmT. We initially set out to test the function of AdmT *in vivo* by overexpressing AdmT in *E. coli* BL21 cells. A disk diffusion antibiotic assay clearly showed notable resistance to andrimid in comparison with *E. coli* cells containing an empty expression vector (Fig. 2*A*), indicating that AdmT can efficiently recruit *E. coli* AccA *in vivo* and form an active heterotetrameric [$(AccA)_2(AdmT)_2$] CT that is less sensitive to andrimid. This observation prompted us to overproduce AdmT with AccA for subsequent *in vitro* characterization. The overproduction of the AccA/AdmT complex was carried out as described previously for AccA/AccD (11). The *accA* and *admT* genes were cloned as a single operon on the basis of the template of *accA*/*accD* genes in pET16b vector to allow for the stoichiometric expression of both proteins (see *Materials and Methods*). Purification relied on the polyhistidine tag encoded at the N terminus of AccA on nickel-nitrilotriacetic acid (Ni-NTA) agarose (Fig. 2*B*). Both AccA/AccD and AccA/AdmT complexes yielded >20 mg of soluble proteins per liter of *E. coli* culture and diminished the potential endogenous *E. coli* AccA binding to <0.1% (11, 16).

The activity of the overproduced AccA/AdmT complex was subsequently assessed spectrophotometrically on the basis of the reverse reaction, CT-catalyzed decarboxylation of malonyl-CoA (see *Materials and Methods*). Biocytin (in excess) was used as a BCCP surrogate (11, 16). The production of acetyl-CoA was coupled to the citrate synthase/malate dehydrogenase reaction cycle, which requires NAD^+ reduction and was monitored at 340 nm (11, 16). Kinetic analyses of AccA/AdmT revealed an apparent K_m of 149 ± 26 μM for malonyl-CoA and 5.1 ± 0.5 mM for biocytin, indicating that the purified AccA/AdmT forms an active CT with catalytic efficiency comparable to that of the *E. coli* AccA/AccD pair (6, 11). The sensitivity of AccA/AdmT to andrimid was tested *in vitro* by IC_{50} measurement. In contrast to *E. coli* AccA/AccD with an IC_{50} value of 12 nM to andrimid, AccA/AdmT complex is nearly 50-fold more resistant to andrimid (IC_{50} = 500 nM) (Fig. 2*C*). The result correlates with the *in vivo* disk assay qualitatively, validating that AdmT is an andrimid-resistant CT β-subunit.

Identification of the Amino Acid Determinant in AdmT That Contributes to Andrimid Resistance. Having established that AdmT constitutes an active CT β-subunit that is resistant to andrimid both *in vivo* and *in vitro*, we sought to examine the underlying molecular mechanism. AdmT shares close homology to *E. coli* AccD with a 36 amino acid residue difference along the 306-residue-length polypeptide chain (Fig. 3*A*), which opened the question of whether a particular (set of) amino acid residue(s) is (are) important for the resistance.

A 3.2-Å resolution x-ray crystal structure of *E. coli* CT, recently disclosed by Waldrop and coworkers (17), served as the entry point for us to approach this problem. Although the available *E. coli* AccA/AccD structure was solved without any substrate, the knowledge gained in the structural studies of other biotin-dependent carboxylases, including *Saccharomyces cerevisiae* and *Streptomyces coelicolor* CTs (18, 19), allows portrayal of the *E. coli* CT catalytic platform as the interfacial six-helix bundle region between its α- and β-subunits. Amino acid residues from Leu-174 to Leu-212 in the AccD polypeptide chain constitute the catalytic region in the CT β-subunit (Fig. 3*B*). Among the 36 amino acid residues that are different between AccD and AdmT, only four fall in the putative catalytic site (Fig. 3). Because andrimid has been determined to be a competitive inhibitor of malonyl-CoA (6), we envisaged that any of the four amino acids mentioned above (Asn-200, Leu-203, Leu-210, and Gly-211) could play a key role in andrimid resistance. Six AdmT mutants were generated through single and double amino acid substitutions that corresponded to the residues of *E. coli* AccD (Table 1, entries 2–7). The andrimid sensitivity of the resulting AdmT variants was assessed qualitatively in *E. coli* BL21 cells by using the disk diffusion antibiotic assay.

AdmT variants harboring the L203M substitution became notably more sensitive to andrimid (Table 1, entries 2 and 4), whereas the alteration of the remaining three residues (Asn-200, Leu-210, and Gly-211) did not produce any apparent effects (Table 1, entries 3 and 5–7). This observation was validated further by using the *in vitro* inhibition assay. AdmT mutants were overproduced in *E. coli* with AccA and purified to homogeneity. IC_{50} measurements revealed that AccA/AdmT(L203M) and AccA/AdmT(N200D/L203M) are both 5 times more sensitive to andrimid than the wild-type (WT) AccA/AdmT complex (IC_{50} = 500 nM) (Table 1, entries 1, 2, and 4). In contrast, the IC_{50} of the other AdmT mutants remained unchanged (Table 1, entries 5–7).

With this quantification of the role of L203M mutation in AdmT on its susceptibility to andrimid, we then sought to test whether the reverse introduction of such a mutation into the WT *E. coli* AccD would result in increased tolerance for the antibi-

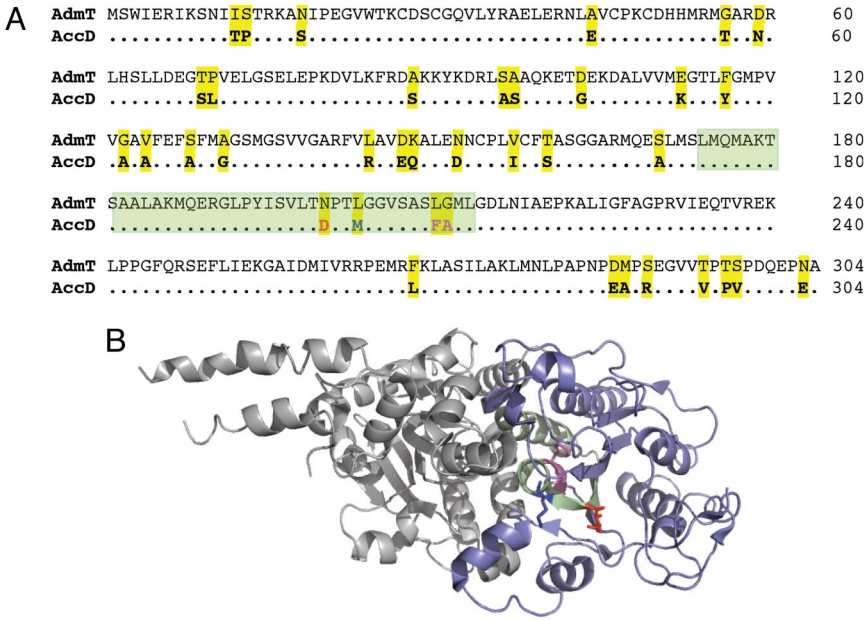

Fig. 3. Bioinformatic mapping of potential amino acid residues in AdmT that confer resistance to andrimid on the basis of its sequence homology with *E. coli* AccD. (*A*) Complete sequence alignment of AdmT with *E. coli* AccD. The putative active sites (Leu-174–Leu-214) in AccD are highlighted in light green, where only four amino acid residues differ from each other. (*B*) Crystal structure of *E. coli* AccA/AccD modeled with PyMol. Color highlights: AccD domain, light purple; active sites (Leu-174–Leu-214), light green; Asp-200, red; Met-203, dark blue; Phe-210 and Ala-211, pink.

otic. Again, we resorted to the disk diffusion antibiotic assay, which allowed direct visual assessment of the sensitivity of WT AccD and their mutants to andrimid. Resistance was clearly observed around the assay disk with 2.5–7.5 μg of andrimid deposited, when the *E. coli* cells were overexpressed with AccD(M203L), compared with AccD(WT) (Table 1, entries 8 and 9). A similar resistance effect was observed when *E. coli* overexpressed AccD(S207Y) (Table 1, entry 10), a mutation identified in an andrimid-resistant *E. coli* strain that was previously created intentionally by serial transfers of growing cultures at sublethal antibiotic concentrations (6). AccD(M203L) and AccD(S207Y) were subsequently overproduced in *E. coli* with AccA for the *in vitro* inhibition assay. IC_{50} measurements further validated again andrimid resistance, because AccD(M203L) and AccD(S207Y) increased ≈5- and 8-fold in resistance (IC_{50} = 55 and 95 nM, respectively), compared with AccD(WT) (IC_{50} = 12 nM) (Table 1, entries 8–10).

Along with the *in vitro* inhibition assays, kinetic analyses of the overproduced CTs and their mutants refined the effects of the mutations on the functions of these enzymes (Table 2). Although all overproduced CTs shared a similar apparent K_m for malonyl-CoA, their catalytic efficiencies varied: the k_{cat}/K_m values of AdmTs containing the L210F mutation and AccD(S207Y) were ≈6-fold lower than those of the WT AdmT and AccD subunits. Inspection of the x-ray crystal structure of *E. coli* AccA/AccD revealed that the Ser-207 residue in AccD and Leu-210 residue in AdmT are not surface-exposed but, rather, buried inside the presumptive catalytic pocket [supporting information (SI) Fig. S1].

Table 1. Identification of a key amino acid residue (Leu-203) in AdmT contributing to andrimid resistance and assessment of this alternation to WT AccD: Disk diffusion (*in vivo*) and IC_{50} (*in vitro*) assays

Entry	AdmT and AccD (WT or mutant)	Disk diffusion assay IZ diameter, mm/andrimid amount, μg*	*In vitro* inhibition assay IC_{50}, nM†
1	AdmT(WT)	<0.5/10; <0.5/15	500
2	AdmT(L203M)	4/10; 6/15	100
3	AdmT(N200D)	<0.5/10; <0.5/15	NA‡
4	AdmT(N200D/L203M)	4/10; 7/15	100
5	AdmT(L210F)	<0.5/10; <0.5/15	1000
6	AdmT(G211A)	<0.5/10; <0.5/15	500
7	AdmT(L210F/G211A)	<0.5/10; <0.5/15	500
8	AccD(WT)	3/2.5; 4/5; 6/7.5	12
9	AccD(M203L)	<0.5/2.5; <0.5/5; <0.5/7.5	55
10	AccD(S207Y)	<0.5/2.5; 1/5; 1/7.5	95

*The disk diffusion assay was carried out by spraying *E. coli* BL21 cells overexpressing *admT* or *accD* (WT or mutant) genes to an andrimid-predeposited LB agar plate (*Materials and Methods*). Inhibition zone (IZ) diameter was measured manually as the nearest point from the disk at which a prominent reduction of bacteria growth occurred.

†IC_{50} measurement was carried out by using recombinantly produced AccA/AdmT and AccA/AccD (WT or mutant) protein complex. For protein overproduction and isolation, see *Materials and Methods*.

‡AccA/AdmT(N200D) could not be reconstituted *in vitro* as a stable protein complex.

BIOCHEMISTRY

Table 2. Kinetic parameters for malonyl-CoA at a fixed concentration of biocytin (5 mM) of WT AccA-AccD (AD), AccA/AdmT (AT), and their mutants

AccD and AdmT mutants	K_m, μM	k_{cat}, min^{-1}	k_{cat}/K_m, $min^{-1}\cdot\mu M^{-1}$
AD(WT)	119 ± 18	751 ± 82	6.31
AT(WT)	148 ± 26	845 ± 89	5.71
AD(M203)	138 ± 24	686 ± 92	4.97
AD(S207Y)	140 ± 28	125 ± 18	0.89
AT(L203)	163 ± 32	954 ± 103	5.86
AT(N200D/L203M)	116 ± 17	718 ± 78	6.19
AT(L210F)	144 ± 23	112 ± 11	0.79
AT(G211A)	146 ± 29	632 ± 84	4.33
AT(L210F/G211A)	134 ± 21	109 ± 15	0.81

Alteration of such residues might have an effect on the conformation of the intersubunit active site and, thereby, the catalytic efficiency. In contrast, the Leu-203 residue in AccD (or Met-203 in AdmT) is located on the protein surface (Fig. S1)

Identification of Other Andrimid-Resistant Bacterial Strains. We envisioned that the 203-Met↔Leu switch in AdmT and AccD might be used as a probe for the identification of other andrimid-resistant bacterial strains. Accordingly, a protein BLAST search using AdmT amino acid sequence 191–214 was performed and allowed for the identification of >10 bacterial strains, the AccD sequences of which have the signature 203MGGVSAV209 motif (details not shown). In particular, several *Vibrio cholerae* strains (*V. cholerae* 1587, 623-39, and MZO-3) have the distinctive Met-203 residue in their AccDs, whereas other *V. cholerae* strains such as N16961 have the Leu-203 residue (Fig. 4*A*). A subsequent disk diffusion assay showed that *V. cholerae* N16961 was sensitive to andrimid, whereas *V. cholerae* 1587, 623-39, and MZO-3 are resistant. (Fig. 4*B*, typical results shown).

Discussion

The emergence of antibiotic-resistant microbial pathogens, as a destined fate of the persistent usage of antibiotics in modern-day living, requires constant effort to discover new antibiotics and understand the mechanisms of antibiotic resistance. Prominent examples of antibiotic-resistant microbes are the native antibiotic producers themselves. They are excellent models for studying antibiotic-resistance mechanisms because producing organisms evolve their own survival strategies to avoid self-destruction during antibiotic biosynthesis. Although the majority of the self-protective strategies exploited by antibiotic-producing microbes involve intracellular antibiotic modification, cellular target modification, and antibiotic efflux (20–22), several antibiotic producers have been known to encode antibiotic-resistant target enzymes that contribute to their survival. The bacterial producers of DNA gyrase inhibitors such as aminocoumarins and albicidins are known to encode DNA gyrase-resistant genes that contribute to their self-protection (23, 24–26), although the molecular mechanism underlying these resistances is still unknown. The D-cycloserine producer *Streptomyces lavendulae* has been shown to encode an antibiotic-resistant alanine racemase (ALR) that manifests a slower enzymatic conversion to the final cycloserine pyridoxal derivatives that inhibit the catalytic activity of ALR (27, 28).

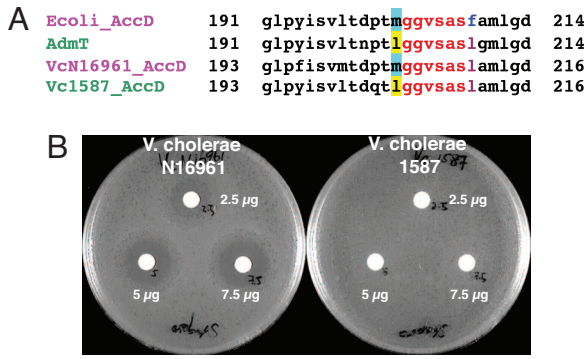

Fig. 4. Identification of andrimid-resistant *V. cholerae* strains by using 203-Met↔Leu substitution in AdmT and AccD as probe. (*A*) Partial sequence alignment of AccD (*E. coli*): AdmT with AccDs of *V. cholerae* N16961 and 1587 indicates that *V. cholerae* strain 1587 would be resistant to andrimid. (*B*) Andrimid-sensitivity assay of *V. cholerae* strains N16961 and 1587 confirms that Vc1587 is resistant to andrimid (assay disks were deposited with 2.5, 5.0, and 7.5 μg of andrimid, respectively).

Andrimid and moiramide belong to a novel class of natural products with a pseudopeptide pyrrolidinedione backbone. They were identified recently as first-in-class potent inhibitors of the bacterial ACC via specific blockade of the CT-catalyzed half-reaction with nanomolar potency (6). Subsequent structure–activity relationship studies led to analogues with modified pseudopeptide motifs and improved efficacies *in vivo* and *in vitro* (29, 30). However, a detailed picture of their interactions with the target bacterial CTs in the first committed step of fatty acid biosynthesis remains elusive.

In this work, we studied the function of the *admT* gene encoded in the andrimid biosynthetic gene cluster and demonstrated that AdmT constitutes an andrimid-resistant form of the CT β-subunit and contributes to the survival of *P. agglomerans* during the production of andrimid. Initial development of an *in vivo* assay, by overexpressing AdmT in *E. coli* cells coupled with the disk diffusion antibiotic assay, allowed for direct visual examination of its andrimid-resistant nature. Subsequent overproduction of AdmT in *E. coli* by coexpression with *E. coli* AccA reconstituted an *in vitro* active heterotetrameric $(AccA)_2(AdmT)_2$ protein complex. Inhibition assays by IC_{50} measurement quantitated the resistant nature of AdmT; its IC_{50} (500 nM) is ≈50 times more than that of AccD (12 nM).

Guided by the x-ray crystal structure of *E. coli* AccA/AccD (17), we focused on the four amino acid residue differences between AdmT and AccD that fall in the putative catalytic center of *E. coli* CT. Mutagenesis studies, coupled with the established *in vivo* and *in vitro* assays, allowed us to identify that the L203M mutation in AdmT confers a 5-fold andrimid-sensitivity recovery. Introduction of such a mutation in a reverse fashion to the WT *E. coli* AccD in turn gave a 5-fold increase in andrimid resistance. It is noteworthy that the AccD(M203L) mutant has an andrimid-resistant profile (i.e., IC_{50}) that is comparable with that of AccD(S207Y), a mutant previously isolated by serial passing of sublethal concentration of an andrimid analogue to *E. coli* cultures (6). Structure modeling of *E. coli* AccA/AccD suggests that the Met-/Leu-203 residue in AccD or AdmT is surface-exposed. Because this residue also locates next to Gly-204-Gly-205, which are postulated to stabilize the anionic intermediate involved in carboxyl-transfer process of the CT-catalyzed reaction (17, 18), it is reasonable to speculate that the Met-/Leu-203 residue in AccD or AdmT is an important residue for the interaction with andrimid or substrate acetyl-CoA.

The L203M substitution in AdmT, however, does not fully mirror the andrimid-resistance profiles of AdmT in comparison with AccD. Additive and cooperative effects of other key residues around the AdmT catalytic core are likely responsible for such discrepancy. A valuable insight will assuredly be provided by the x-ray cocrystal structures of AccA/AdmT and AccA/AccD complexed with andrimid.

The recognition of Met↔Leu switches in AccD and AdmT in modulating sensitivities to andrimid allowed us to use it as a signature probe to identify several *V. cholerae* bacterial strains

that, on examination, are resistant to andrimid. By close examination of the genomes of these *V. cholerae* strains, it was noticed that all of the andrimid-sensitive strains encode two CT β-subunit genes, among which one is predictively resistant to andrimid but the other is sensitive. The andrimid gene clusters from *P. agglomerans* (14) and *Vibrionales* SWAT-3 (5) both encode transposases at the boundaries of the clusters that are likely responsible for horizontal gene transfer (HGT). Although this fact may explain the wide distribution of andrimid- and moiramide-producing Gram-negative bacteria in diverse ecological niches, it also suggests that the resistant *accD* genes that occur in several *V. cholerae* strains may have been acquired through HGT. The emergence of andrimid resistance, through HGT and as shown here by simple point mutation, raises likely resistance pathways for andrimid and derivatives if they progress to clinical development. Understanding the molecular interactions of the pseudopeptide pyrrolidinedione molecules with bacterial CT targets will be critical in the development of efficacious andrimid derivatives that are less susceptible to such a self-protective mechanism of antibiotic resistance.

Materials and Methods

Materials. Andrimid was isolated from *P. agglomerans* as described previously (14), and the purity (>95%) was determined by HPLC and ^{1}H NMR analysis. L-Malate, biocytin, malonyl-CoA, NAD, BSA, L-malate dehydrogenase (from porcine heart), and citrate synthase (from porcine heart) were purchased from Sigma. *E. coli* BL21 DE3 cells (for protein overproduction) were purchased from Invitrogen. *E. coli* NovaBlue DE3 cells (for general cloning purpose) and pET-16b plasmid were obtained from Novagen. pQTev plasmid was obtained from the Protein Structure Factory.

Cloning. *accD* and *admT* genes were amplified from plasmid pSJ9 (12) and cosmid 2194C1 (14) by using primers 1–3 (Table S1) and ligated into the BglII and NotI sites of expression vector pQTev to give plasmids pXL90 and pXL91. For the *in vitro* assay of AccD and AdmT activities, they were cloned as one operon with the *E. coli accA* gene, respectively. A chimeric *accA/accD* gene containing an XhoI restriction site and a ribosomal binding site in between was first constructed as described previously (11). In brief, *accA* and *accD* genes were amplified from plasmids pLS151 (31) and pSJ9 by using primers 4–7 (Table S1) and overlap-extended by using primers 4 and 7 to give the target chimeric *accA/accD* gene. This gene was ligated into the NdeI and BamHI sites of expression vector pET16b to give plasmid pXL92. The *admT* gene was then amplified from cosmid 2194C1 by using primers 8 and 9 (Table S1) and ligated to the XhoI and BamHI sites of pXL92 to give plasmid XL93.

Site-Directed Mutagenesis. The mutants of AccD and AdmT for *in vivo* and *in vitro* bioassays were generated by using a Stratagene QuikChange Multi site-directed mutagenesis kit with plasmids pXL90–pXL93 as the templates and primers 10–17 (Table S1).

***In Vivo* Assay for Andrimid Sensitivity.** *E. coli* BL21 DE3 cells were transformed with pXL90, pXL91, and their mutant derivatives and grown in LB medium supplemented with ampicillin (100 μg/ml). Cells were grown at 37°C to an OD_{600} of $\approx$0.6 and then induced at 30°C with 1 mM isopropyl β-D-thiogalactoside and grown for an additional 4 h at 30°C. The expression levels of the AdmT or AccD (WT and mutant) proteins were assessed by SDS/PAGE and determined to be similar in all cell-culture extracts. Varied amounts of andrimid (5 mg/ml in DMSO) were deposited on the blank sterile concentration disk (Difco) on LB agar plates containing ampicillin (100 μg/ml). The plates were then oversprayed with the 1:100 (vol/vol) aqueous dilution of the induced *E. coli* culture and incubated at 30°C overnight and at room temperature for 2 days. Plate images were acquired by using a multilight imager (Alpha Innotech). Inhibition-zone diameters were measured manually and defined as the nearest point from the disk at which a visible reduction of bacterial growth occurred. For *V. cholerae* strains, the andrimid-spotted LB agar plates were oversprayed with 1:100 (vol/vol) aqueous dilution of the overnight-grown *V. cholerae* cell cultures. The plates were then incubated at 30°C overnight, and images were acquired accordingly.

Protein Overproduction. The His-tagged AccA/AccD, AccA/AdmT, and their mutant protein complexes were overproduced in *E. coli* BL21 DE3 in a manner analogous to that described previously (11). The proteins were purified to apparent homogeneity by Ni-NTA agarose column and buffer-exchanged to 25 mM Hepes (pH 7.5) and 500 mM NaCl. Protein concentrations were determined by using the Bradford assay. Proteins were aliquot-flash-frozen in liquid nitrogen and stored at −80°C. The overproduction yields for each protein were typically 20–25 mg/liter.

***In Vitro* CT Activity and Inhibition Assay.** The CT activity was monitored in the reverse direction, where the production of acetyl-CoA from malonyl-CoA was coupled to the citrate synthase/malate dehydrogenase reaction cycle leading to the NAD^+ reduction (16). The assay was performed at room temperature in 96-well microtiter plates, and the reaction was monitored spectrophotometrically at 340 nm after the formation of NADH. A typical reaction mixture (100 μl) contained 100 mM Tris·Cl (pH 8.0), 10 mM L-malate, 0.5 mM NAD^+, 0.6 mg of BSA, 6.8 units/ml (0.1 mg/ml) citrate synthase, 3.6 units/ml (0.07 mg/ml) malic dehydrogenase, biocytin (standard assay concentrations, 5 mM) and malonyl-CoA (standard assay concentration, 0.1 mM). The reaction was initiated by the addition of CT. To determine the kinetic parameters of the enzymatic reaction, initial velocities were obtained by varying the substrate concentrations (biocytin and malonyl-CoA). The data were calculated by nonlinear regression of initial velocity values and substrate concentrations and fit to the Michaelis–Menten equation by using GraphPad Prism 5 software (GraphPad Software). For andrimid-inhibition assays, the initial velocity of the enzyme activities was determined in the presence of various concentrations of andrimid under standard assay conditions. IC_{50} values were obtained by fitting the data to a sigmoid dose–response equation by using the GraphPad Prism software.

ACKNOWLEDGMENTS. We thank Prof. John Cronan (Department of Microbiology, University of Illinois, Urbana–Champagne), for providing plasmids pLS151 and pSJ9 that encode *E. coli accA* and *accD* genes, and Prof. John Mekalanos (Department of Microbiology and Molecular Genetics, Harvard Medical School), for providing the *V. cholerae* strains used in this study. This work was supported in part by National Institute of Health Grant GM20011 (to C.T.W.) and the Swiss National Science Foundation and Ernst Schering Foundation (postdoctoral fellowships to X.L.).

1. Walsh CT (2003) Where will new antibiotics come from? *Nat Rev Microbiol* 1:65–70.
2. Fredenhagen A, *et al.* (1987) Andrimid, a new peptide antibiotic produced by an intracellular bacterial symbiont isolated from a brown planthopper. *J Am Chem Soc* 109:4409–4411.
3. Needham J, Kelly MT, Ishige M, Andersen RJ (1994) Andrimid and moiramides A-C, metabolites produced in culture by a marine isolate of the bacterium *Pseudomonas fluorescens*: Structure elucidation and biosynthesis. *J Org Chem* 59: 2058–2063.
4. Oclarit JM, *et al.* (1994) Anti-bacillus substance in the marine sponge, *Hyatella* species, produced by an associated *Vibrio* species bacterium. *Microbios* 78:7–16.
5. Long RA, *et al.* (2005) Antagonistic interactions among marine bacteria impede the proliferation of *Vibrio cholerae*. *Appl Environ Microbiol* 71:8531–8536.
6. Freiberg C, *et al.* (2004) Identification and characterization of the first class of potent bacterial acetyl-CoA carboxylase inhibitors with antibacterial activity. *J Biol Chem* 279:26066–26073.
7. Cronan JE, Jr, Waldrop GL (2002) Multi-subunit acetyl-CoA carboxylases. *Prog Lipid Res* 41:407–435.
8. Choi-Rhee E, Cronan JE, Jr (2003) The biotin carboxylase-biotin carboxyl carrier protein complex of *Escherichia coli* acetyl-CoA carboxylase. *J Biol Chem* 278:30806–30812.
9. Janiyani K, Bordelon T, Waldrop GL, Cronan JE, Jr (2001) Function of *Escherichia coli* biotin carboxylase requires catalytic activity of both subunits of the homodimer. *J Biol Chem* 276:29864–29870.
10. Li SJ, Cronan JE, Jr (1992) The gene encoding the biotin carboxylase subunit of *Escherichia coli* acetyl-CoA carboxylase. *J Biol Chem* 267:855–863.
11. Blanchard CZ, Waldrop GL (1998) Overexpression and kinetic characterization of the carboxyltransferase component of acetyl-CoA carboxylase. *J Biol Chem* 273:19140–19145.
12. Li SJ, Cronan JE, Jr (1992) The genes encoding the two carboxyltransferase subunits of *Escherichia coli* acetyl-CoA carboxylase. *J Biol Chem* 267:16841–16847.
13. Campbell JW, Cronan JE, Jr (2001) Bacterial fatty acid biosynthesis: Targets for antibacterial drug discovery. *Annu Rev Microbiol* 55:305–332.
14. Jin M, Fischbach MA, Clardy J (2006) A biosynthetic gene cluster for the acetyl-CoA carboxylase inhibitor andrimid. *J Am Chem Soc* 128:10660–10661.
15. Fortin PD, Walsh CT, Magarvey NA (2007) A transglutaminase homologue as a condensation catalyst in antibiotic assembly lines. *Nature* 448:824–827.
16. Guchhait RB, *et al.* (1974) Acetyl coenzyme-A carboxylase system of *Escherichia coli*: Purification and properties of biotin carboxylase, carboxyltransferase, and carboxyl carrier protein components. *J Biol Chem* 249:6633–6645.

17. Bilder P, *et al*. (2006) The structure of the carboxyltransferase component of acetyl-CoA carboxylase reveals a zinc-binding motif unique to the bacterial enzyme. *Biochemistry* 45:1712–1722.
18. Diacovich L, *et al*. (2004) Crystal structure of the beta-subunit of acyl-CoA carboxylase: Structure-based engineering of substrate specificity. *Biochemistry* 43:14027–14036.
19. Zhang HL, Yang ZR, Shen Y, Tong L (2003) Crystal structure of the carboxyltransferase domain of acetyl-coenzyme a carboxylase. *Science* 299:2064–2067.
20. Walsh CT (2003). *Antibiotics: Action, Origins, Resistance* (Am Soc Microbiol, Washington, DC).
21. Hopwood DA (2007) How do antibiotic-producing bacteria ensure their self-resistance before antibiotic biosynthesis incapacitates them? *Mol Microbiol* 63:937–940.
22. Cundliffe E (1989) How antibiotic-producing organisms avoid suicide. *Annu Rev Microbiol* 43:207–233.
23. Schmutz E, Muhlenweg A, Li SM, Heide L (2003) Resistance genes of aminocoumarin producers: Two type II topoisomerase genes confer resistance against coumermycin A(1) and clorobiocin. *Antimicrob Agents Chemother* 47:869–877.
24. Thiara AS, Cundliffe E (1993) Expression and analysis of two Gyrb genes from the novobiocin producer, *Streptomyces sphaeroides*. *Mol Microbiol* 8:495–506.
25. Thiara AS, Cundliffe E (1989) Interplay of novobiocin-resistant and novobiocin-sensitive DNA gyrase activities in self-protection of the novobiocin producer, *Streptomyces sphaeroides*. *Gene* 81:65–72.
26. Thiara AS, Cundliffe E (1988) Cloning and characterization of a DNA gyrase B-gene from *Streptomyces sphaeroides* that confers resistance to novobiocin. *EMBO J* 7:2255–2259.
27. Noda M, Matoba Y, Kumagai T, Sugiyama M (2004) Structural evidence that alanine racemase from a D-cycloserine-producing microorganism exhibits resistance to its own product. *J Biol Chem* 279:46153–46161.
28. Noda M, *et al*. (2004) Self-protection mechanism in D-cycloserine-producing *Streptomyces lavendulae*: Gene cloning, characterization, and kinetics of its alanine racemase and D-alanyl-D-alanine ligase, which are target enzymes of D-cycloserine. *J Biol Chem* 279:46143–46152.
29. Pohlmann J, *et al*. (2005) Pyrrolidinedione derivatives as antibacterial agents with a novel mode of action. *Bioorg Med Chem Lett* 15:1189–1192.
30. Freiberg C, Fischer HP, Brunner NA (2005) Discovering the mechanism of action of novel antibacterial agents through transcriptional profiling of conditional mutants. *Antimicrob Agents Chemother* 49:749–759.
31. Li SJ, Rock CO, Cronan JE, Jr (1992) The DedB (Usg) open reading frame of *Escherichia coli* encodes a subunit of acetyl-coenzyme A carboxylase. *J Bacteriol* 174:5755–5757.